Measurement and Calculation of Electric Field Gradients in Hg-Mercaptides*

Torsten Soldner**, Wolfgang Tröger, Tilman Butz, Peter Blaha[a], Karlheinz Schwarz[a] and the ISOLDE-Collaboration[b]

Abteilung Nukleare Festkörperphysik, Universität Leipzig, Linnéstraße 5, D-04103 Leipzig
[a] Institut für Technische Elektrochemie, Technische Universität Wien, Getreidemarkt 9/158, A-1060 Wien
[b] CERN, CH-1211 Genève 23, Switzerland

Z. Naturforsch. **53a**, 404–410 (1998); received October 31, 1997

Electric field gradients (EFG) at Hg were determined in mercury mercaptides $Hg(S(CH_2)_iCH_3)_2$ experimentally for $i \in \{0, 1, 2\}$ using time differential perturbed angular correlation and theoretically for $i \in \{0, 1\}$ with the full potential linearized augmented plane wave code WIEN95. Due to the large unit cells and small hydrogen atoms not full convergence of the plane wave basis set could be reached. Nevertheless, the calculated EFGs agree with experimental values to better than 20%. Furthermore, isolated molecules for $i \in \{0, 1\}$ were investigated theoretically, and strong differences to the values for the crystalline state, especially for the asymmetry parameters η, were found.

1. Introduction

The mercury-thiolate chemistry is dominated by an almost linear twofold ligation of Hg^{2+} by thiols (–S–Hg–S–). This holds also true for the interaction of thiol containing biomolecules like the amino acid cysteine with its thiol side chain. Unfortunately, biological systems are too complicated to start the investigation of S–Hg–S bonds. Simpler model compounds with S–Hg–S bonds are mercury mercaptides such as $Hg(S(CH_2)_iCH_3)_2$, $i \in \{0, 1, 2, \ldots\}$. These organometallic compounds allow to study the Hg^{2+}-binding by thiols via the detection of the electric field gradient at the Hg^{2+}-site by time differential perturbed angular correlation (TDPAC). Furthermore, the relatively simple crystal structure of the "shorter" mercaptides allows to calculate the EFG at Hg sites.

We systematically investigated the mercury mercaptides for $i \in \{0, 1\}$ both experimentally and theoretically, and for $i = 2$ experimentally. The experiments were carried out using the TDPAC of γ-rays from the short-lived mercury isotope ^{199m}Hg. The calculations were performed for the crystal structures described in [1, 2] as well as for isolated molecules derived from these crystal structures.

The full potential linearized augmented plane wave (FPLAPW) method as embodied in the program package WIEN95 [3] has proven to be an accurate and powerful method to calculate electron densities and electric field gradients in crystals [4]. It comes to its limits when applied to crystals with large unit cells and atoms exhibiting short bonding distances, both occurring in organometallic compounds. Mercury mercaptides are ideally suited to check these limits and to get an insight into the possibilities to overcome them by simplifying the description of the chemical bond because cut-off effects can be tested directly by varying the number of the CH_2-groups (e.g., $i \in \{0, 1, 2\}$).

2. Experimental

2.1 Method

For the TDPAC measurements the 374 keV–158 keV γ-γ-cascade of ^{199m}Hg ($\tau_{1/2} = 43$ min) was used. The half-life of the intermediate state ($I = 5/2$, $Q = 0.674(77)$ barn [8]) is 2.3 ns only. Furthermore, the 375 keV transition is highly converted (total conversion coefficient $\alpha_{tot} = 5$). Therefore these measurements require an extremely efficient spectrometer with excellent time resolution such as the six detector TDPAC camera described in [5]. The time resolution of the TDPAC camera τ_{FWHM} was about 650 ps.

Assuming one binding site for ^{199m}Hg, the time spectra were fitted using the function G_{22} given as [6]

$$G_{22}(t) = \text{amp} \sum_i a_i(\eta) \exp(-0.09\, \tau^2_{FWHM}(\omega_i(\eta)\, t)^2) \cdot \exp(-\delta\, \omega_i(\eta)\, t) \cos(\omega_i(\eta)\, t) + \text{const}, \quad (1)$$

* Presented at the XIVth International Symposium on Nuclear Quadrupole Interactions, Pisa, Italy, July 20–25, 1997.

** Present address: Physik-Department E21, Technische Universität München, James-Franck-Straße, D-85748 Garching, Germany.

Reprint requests to T. Butz, Fax: +49-341-9732748.

0932-0784 / 98 / 0600-0404 $ 06.00 © – Verlag der Zeitschrift für Naturforschung, D-72027 Tübingen

where τ_{FWHM} is the full width at half maximum value of the spectrometer time resolution function, ω_1 the precession frequency, and δ the half width at half maximum of the inhomogeneous Lorentz-type line broadening. The $a_i(\eta)$ are theoretically determined η-dependent amplitudes. Furthermore, a time independent amplitude (amp) and base-line (const.) are allowed to take into account the source-detector geometry effects due to different sample volumes and possible detector-sample missalignment.

2.2 Sample Preparation

Wertheim's method [7] was used for the sample preparation and adapted to the special requirements.

The mercaptans were purchased from Fluka. ^{199m}Hg, produced at the mass separator ISOLDE (CERN), was implanted into ice. The ice was molten. An aliquot of 0.5 ml of the mercaptan (purum) was dissolved in 1 ml ethanol (mercaptan concentration: ≈ 5 M, mercaptan: ≈ 7 mmol). The mercaptan and the ethanol were cooled to $-70\,^{\circ}$C in order to avoid losses by evaporation. 200 µl of the solution were mixed with 300 µl of the ^{199m}Hg solution. 100 µl to 400 µl of a 10% (mass) solution of $Hg(CN)_2$ (Hg concentration 0.4 M, Hg: 40 µmol ... 120 µmol) was added as carrier. The precipitate was centrifuged for 10 min at $\approx 4000\,g$ and the supernatant carefully removed; this procedure was carried out twice. About 70% to 90% of the ^{199m}Hg activity was found in the precipitate. The pellet of the precipitated mercaptide was used for the TDPAC measurements at room temperature.

In experiments in which the mercaptans were incubated with the ^{199m}Hg activity with no carrier added, no precipitation was observed. The TDPAC spectra of the frozen mercaptide solutions at 77 K exhibit more than two different NQIs with considerable frequency distributions for all investigated mercaptides, inconsistent with the NQIs found in the experiments were $Hg(CN)_2$ as carrier was added. Obviously, a certain amount of carrier is necessary to avoid the binding of Hg^{2+} to unspecific binding sites in side directions due to insufficient mercaptide purity.

2.3 Results

Figure 1 shows the time and Fourier spectra obtained for all three mercaptides. All spectra could be fitted using (1) assuming a unique probe site. The results are listed in Table 1. The corresponding EFG values are listed in Table 3. For the calculation of the EFGs from the experimental data (precession frequency ω_1 and asymmetry parameter η) the quadrupole moment $Q = 0.674(77)$ barn for the ^{199m}Hg spin 5/2-state [8] was used.

Table 1. NQI in $^{199m}Hg(S(CH_2)_iCH_3)_2$, $i \in \{0, 1, 2\}$.

	Counts 10^6	amp %	δ %	ω $10^9\,s^{-1}$	η
$Hg(SCH_3)_2$	22.44	10.3(3)	0.5(2)	1.181(4)	0.212 (6)
$Hg(SCH_2CH_3)_2$	34.22	9.6(1)	0, fix	1.268(2)	0.084 (9)
$Hg(S(CH_2)_2CH_3)_2$	16.79	9.1(2)	0, fix	1.326(4)	0.089(14)

3. Calculations

3.1 Crystal Structure

The crystal structures determined by Bradley and Kunchur [1, 2] for $Hg(S(CH_2)_iCH_3)_2$, $i \in \{0, 1\}$, were used. Methylmercaptide ($i = 0$) crystallizes in the space group Pbca and exhibits eight formula units per unit cell. The orthorhombic unit cell has the dimensions $a = 37.416(9)$ a.u.[1], $b = 14.32(4)$ a.u., and $c = 14.74(4)$ a.u. [1]. Ethylmercaptide ($i = 1$) and propylmercaptide ($i = 2$) build up monoclinic crystals of the space group Cc with four formula units per unit cell and the unit cell dimensions $a = 14.25(4)$ a.u., $b = 9.20(2)$ a.u., $c = 44.98(8)$ a.u., $\beta = 85°$ [2] and $a = 13.87$ a.u., $b = 9.68$ a.u., $c = 61.98$ a.u., $\beta = 51°$ [7], respectively. Unfortunately, for $i = 2$ no atomic positions were available from literature.

The coordinates of the hydrogen atoms could not be determined by X-ray diffraction [1, 2]. Therefore, for the calculations within the present work, these atoms were placed as in well-known CH_3 or CH_2 groups, assuming a C–H-distance of 2.04 a.u.[2] and a tetrahedral bond angle of 109.4°. The hydrogen atoms were relaxed within a few steps using a damped Newton dynamics [9], proving that the simple assumptions on the hydrogen positions were correct.

Figure 2 contains plots of the unit cells of $Hg(SCH_3)_2$ and $Hg(SCH_2CH_3)_2$.

In the calculations of the isolated molecules, all but one molecule are deleted from the unit cell[3]. This can

[1] In this paper, atomic units are used: 1 a.u. = $5.29177 \cdot 10^{-11}$ m.

[2] This value was obtained by minimizing the total energy for methane (CH_4) in a cubic unit cell of 10 a.u. × 10 a.u. × 10 a.u., using WIEN95.

[3] The periodic unit cell structure is necessary to apply the FPLAPW method.

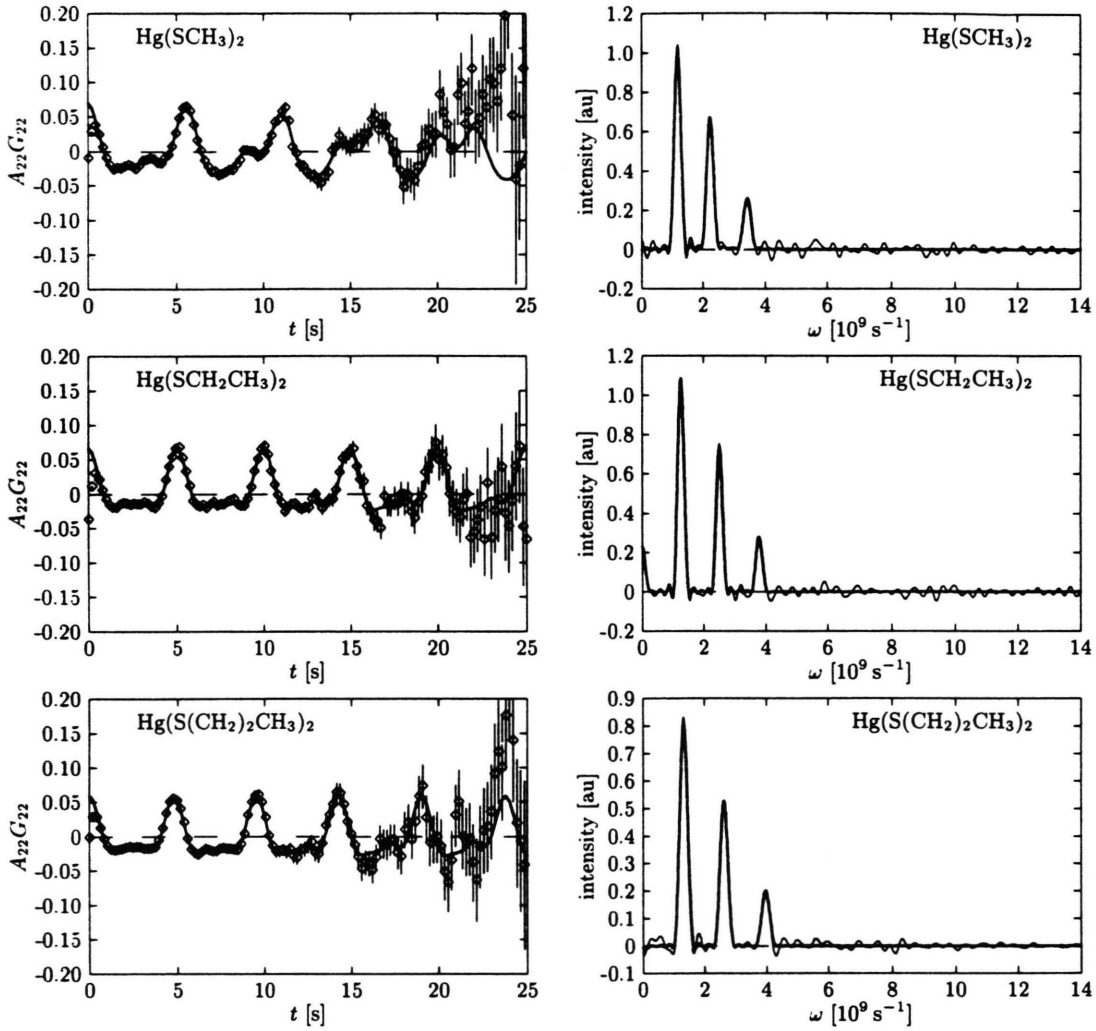

Fig. 1. Time spectra (left) and their Fourier transforms (right) of the TDPAC measurements of $^{199m}Hg(S(CH_2)_iCH_3)_2$, $i \in \{0, 1, 2\}$.

be considered as a fairly good approximation for an isolated molecule, since the unit cells are large. For $Hg(SCH_3)_2$, also two molecules were kept in order to keep inversion symmetry. (Note that inversion symmetry leads to a real symmetric instead of a complex hermitian eigenvalue problem, and this reduces the required computer memory by a factor of two.) In addition, $Hg(SCH_3)_2$ was also placed in a tetragonal unit cell of 20 a.u. × 10 a.u. × 10 a.u. using the same intramolecular distances and angles as in the larger true unit cell. The two latter cases are illustrated in Figure 3. Further changes in the shape of the unit cells were not performed.

3.2 Basis Set

In the FPLAPW method the unit cell is split up into spheres around the atoms and the interstitial region. Inside the spheres, the wave function, potential, and electron density are expanded in spherical harmonics, whereas in the interstitial region plane waves are used (see e.g. [3]).

The quality of the plane wave basis set can be checked by considering the parameter RK_{max} defined as

$$RK_{max} = \min_{\beta} \{R_\beta\} \max_{\boldsymbol{K}} \{|\boldsymbol{K}|\}, \tag{2}$$

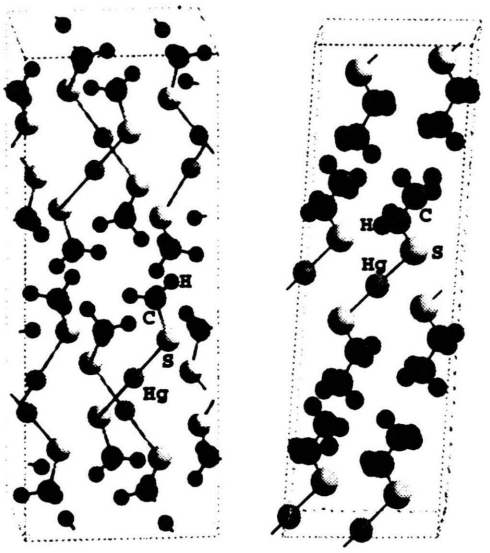

Fig. 2. Unit cells of $Hg(SCH_3)_2$ (left) and $Hg(SCH_2CH_3)_2$ (right).

where R_β is the radius of the sphere β and $\boldsymbol{K}$ runs over the reciprocal lattice vectors. RK_{max} is usually a good measure for the quality of the plane wave basis set because for smaller spheres shorter wave lengths of the plane waves and therefore larger $\boldsymbol{K}$-vectors are necessary. Usually $RK_{max} = 7 \ldots 9$ gives very good convergence, but for systems containing very small H spheres (e.g. 0.6 a.u.) RK_{max} can be significantly reduced.

We tried to test the convergence of the plane wave basis set by increasing RK_{max}, but it turned out that convergence could not be reached for these unit cells due to main memory limitations (300 MByte). Even for $Hg(SCH_3)_2$ in the smaller tetragonal unit cell described above, full convergence could not be reached. The dependence of the total energy, the EFG at the Hg-site, and the forces at the atoms in this tetragonal cell on RK_{max} (for $2.0 \leq RK_{max} \leq 3.0$) is given in Table 2.

Table 2. Test of the convergence parameter RK_{max} for $Hg(SCH_3)_2$ in the tetragonal unit cell. The total energy E is given with respect to the lowest value for $RK_{max} = 3.0$.

RK_{max}	2.0	2.5	3.0
E [Ry]	1.8448	0.2854	0.0000
V_{zz}^{Hg} [10^{21} V/m^2]	−92.1	−83.1	−82.2
η^{Hg}	0.423	0.466	0.469
$\lvert F^S \rvert$ [mRy/a.u.]	119.3	124.2	119.0
$\lvert F^C \rvert$ [mRy/a.u.]	89.5	98.6	85.9
$\lvert F^H \rvert$ [mRy/a.u.]	17.4	12.7	20.3

Table 3 contains EFG values for different RK_{max} values (and structures). This allows an estimation how the EFG evolves with RK_{max}, since more reliable calculations using $RK_{max} = 3-4$ were not possible due to computer limitations.

The necessary number of $\vec{k}$-points in the first Brillouin zone was tested for crystalline $Hg(SCH_3)_2$. From a comparison of the results in Table 3 we conclude that in these molecular crystals one $\vec{k}$-point is sufficient, and this was used in all further calculations.

3.3 Relaxations

Because the hydrogen coordinates were not known experimentally, they were relaxed as described in Subsection 3.1. The influence of the H positions on the EFG at the Hg sites was negligible.

Since in some cases (especially for the isolated molecules) large forces were found, we tried to perform also a relaxation of all other atomic positions. Figure 4 shows the total force (sum of the values of the forces at all atoms) and total energy versus the steps of relaxation for crystalline $Hg(SCH_3)_2$. The total force decreases, as expected, during relaxation, but the total energy shows a non-monotonic behaviour. Table 3 compares EFG values for unrelaxed and relaxed structures with experimental values. In all cases, the

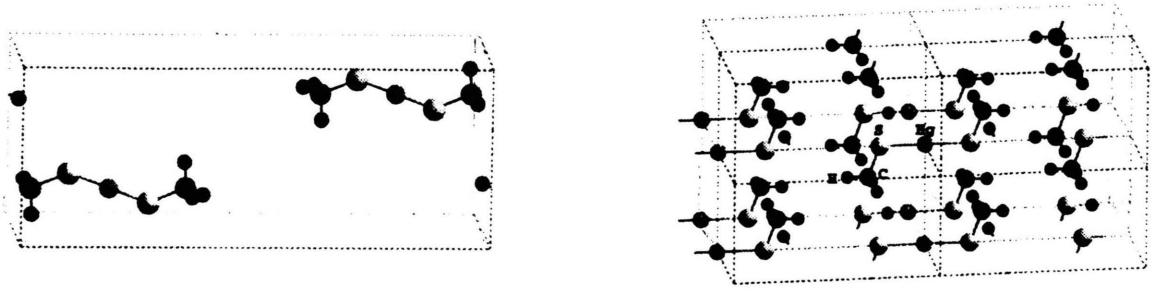

Fig. 3. $Hg(SCH_3)_2$ as quasi-isolated molecule in the crystal cell preserving inversion symmetry (left) and in a tetragonal unit cell (right, eight unit cells are plotted).

Table 3. Experimental and calculated EFG values at Hg-sites in $Hg(S(CH_2)_iCH_3)_2$, $i \in \{0, 1, 2\}$.

Mercaptide		State	RK_{max}	V_{zz}^{Hg} $[10^{21}\ V/m^2]$	η^{Hg}
$Hg(SCH_3)_2$	exp, 293 K	crystalline		±73.4(8.3)	0.212(6)
$Hg(SCH_3)_2$		crystalline	1.75	−90.8	0.181
$Hg(SCH_3)_2$		crystalline	1.75[a]	−89.65	0.203
$Hg(SCH_3)_2$	relaxed	crystalline	1.75	−135.1	0.203
$Hg(SCH_3)_2$		molecule[b]	1.75	−105.4	0.440
$Hg(SCH_3)_2$	relaxed[c,d]	molecule[b]	1.75	−106.2	0.428
$Hg(SCH_3)_2$		molecule	1.75	−105.9	0.441
$Hg(SCH_3)_2$		molecule	1.90	−95.4	0.395
$Hg(SCH_3)_2$	relaxed[d]	molecule	1.90	−101.2	0.353
$Hg(SCH_3)_2$		molecule[e]	2.00	−92.1	0.423
$Hg(SCH_3)_2$		molecule[e]	3.00	−82.2	0.469
$Hg(SCH_2CH_3)_2$	exp, 293 K	crystalline		±81.9(9.4)	0.084(9)
$Hg(SCH_2CH_3)_2$		crystalline	2.00	−83.8	0.033
$Hg(SCH_2CH_3)_2$		crystalline	2.25	−76.0	0.042
$Hg(SCH_2CH_3)_2$		crystalline	2.50	−74.7	0.043
$Hg(SCH_2CH_3)_2$		crystalline	2.75	−73.5	0.047
$Hg(SCH_2CH_3)_2$		molecule	1.85	−83.0	0.464
$Hg(SCH_2CH_3)_2$	relaxed	molecule	1.85	−87.0	0.405
$Hg(S(CH_2)_2CH_3)_2$	exp, 293 K	crystalline		±85.6(9.9)	0.089(14)

[a] 24 $\vec{k}$-points.
[b] With inversion as symmetry operation.
[c] H-positions only.
[d] Relaxation not completed.
[e] In a tetragonal unit cell.

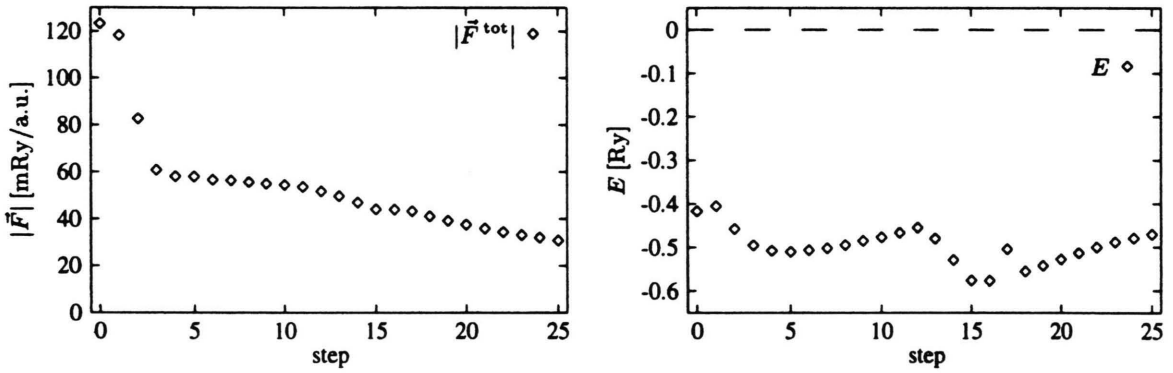

Fig. 4. Total force and energy versus step number for the relaxation calculation of all atomic positions in crystalline $Hg(SCH_3)_2$.

inclusion of relaxation deteriorates the agreement with experiment. Due to this fact, and from our findings in [10] that underconverged basis sets may lead to unreliable (wrong) forces, we consider the obtained relaxations as unreliable.

3.4 Electric Field Gradients

The calculated EFGs in different approximations (crystals and quasi-isolated molecules, different degrees of relaxation, basis set size) are compared with experimental data in Table 3.

4. Discussion

4.1 Experiments

The experimentally obtained NQI parameters according to (1) are summarized in Table 1 (corresponding V_{zz} see Table 3). In addition, the number of coincidence counts of the TDPAC time spectra (see Fig. 1) is given. Because of the excellent statistical quality of the data the time dependent anisotropy could be recorded up to more than 10 half-lifes, i.e. 25 ns. All TDPAC-spectra show one unique NQI within the instrumental linewidth of ≈200 Mrad/s with no additional fre-

quency distribution. Only in the case of methylmercaptide a small frequency distribution of about 0.5% is observed.

No evidence for intramolecular dynamics was found.

The relatively high precession frequencies and the small asymmetry parameters are characteristic for a linear or almost linear coordination of Hg^{2+} by two thiols, other contributions to the EFG from distant azimuthal atoms or molecules being negligibly small. In the case of methylmercaptide there is a larger asymmetry parameter $\eta = 0.212(6)$, and additional line broadening is observed. This indicates that the influence of distant azimuthal atoms or molecules is no longer negligible. The linewidth suggests disorder in the positions of these distant atoms or molecules.

Another interesting feature is the increase of the precession frequency with increasing chain length. In our earlier work on mercury halogenides [8, 10] we found that the Hg-6p states dominate the EFG. These states are almost unoccupied but they contain the orthogonolized tail of the halogen wave function and therefore are called off-site contributions. In the case of the Hg–S bond we expect a similar behaviour and suppose that with increasing chain length, electrons are transferred from Hg to S which increases the off-site contributions. A similar behaviour was found for dimercaptobenzene ($\omega_1 = 1205(6)$ Mrad/s, $\eta = 0.213(10)$) and benzylmercaptan ($\omega_1 = 1341(4)$ Mrad/s, $\eta = 0.127(9)$); In the first compound the thiolgroup is directly linked to a benzol ring, in the latter one via a CH_2 group [11].

Propylmercaptide shows the highest precession frequency $\omega = 1326(4)$ Mrad/s. This frequency corresponds to the frequency of Hg-cysteine $\omega = 1360(16)$ Mrad/s ($\eta = 0.149(17)$). Here, Hg^{2+} is linearly coordinated by the thiolgroups of two cysteines ((COOH)–$CHNH_4$–CH_2–S–Hg–S–CH_2–$CHNH_4$(COOH)) which has the same chain length as propylmercaptide but different endgroups. This supports our hope that in the case of Hg–S bonds complicated structures in biological systems can be simplified in ab initio calculations of EFGs.

4.2 Basis Set

The results for different RK_{max} values in Tables 2 and 3 clearly show that convergence of the plane wave basis set could not be reached in any of the investigated systems. Also for the relatively small tetragonal unit cell the available computer memory was insufficient. The large unit cells in combination with short bonding distances (especially for the C–H bond of about 2 a.u. only) require very large reciprocal lattice vectors and therefore large matrix sizes. Here, the FPLAPW method reaches its limits. Of course, with improved computer hardware and decreasing memory cost the treatment of larger systems is possible in the future.

There can be two solutions of these limitations: i) the use of other methods with different basis sets and, ii) a simplification of the calculated structure, where one tries to calculate the EFG at a particular atom not in the complicated crystal, but in a small fragment centered around the atom of interest (in this case around Hg). The first way was used e.g. by Hemmingsen and Ryde who calculated EFGs in molecular $CdCl_2$ using an LCAO Hartree-Fock-method [12]. Although this method is more suited for molecules, the Gaussian orbital basis set has a poor asymptotic behaviour near the nucleus, and in particular for heavier elements (like Hg) it is very difficult to construct a good Gaussian basis. Therefore the EFG values are probably less accurate than with a FPLAPW basis set (see e.g. [10]). First steps towards the second method were tried for molecules in the present paper. Comparing EFG values for $Hg(SCH_3)_2$ with one or two molecules in the crystal unit cell and with one molecule in the tetragonal unit cell at comparable RK_{max} values shows that the differences are of the same order or smaller than basis set effects (Table 3). This may allow the usage of a smaller unit cell but consequently a much better basis set (higher RK_{max} parameters). For solids, this method is not applicable because the unit cell is small and all interactions between atoms within the unit cell are important. For large molecules (molecular crystals) a simplification such as the replacement of C_xH_y-groups by H or other atoms could be possible. Unpublished test calculations showed that this is a very delicate problem and needs further work [13].

4.3 Relaxation

The calculation of relaxations of hydrogen atoms was successful. Obviously, the assumed coordinates were accurate enough to yield small forces and to allow the hydrogen atoms to reach their equilibrium positions.

The unphysical results of the relaxations of all other atoms have to be related to the insufficient basis set.

The forces could not be calculated with the necessary precision, and therefore the atoms were moved in erroneous directions. For instance the Hg–S bond length in the relaxed structure was only 4.06 a.u., which is unphysically small compared to the experimental distance of 4.46 a.u.

4.4 Electric Field Gradients

In spite of the poor basis set, EFGs could be calculated in acceptable agreement with experimental values: The deviation was 20% for $Hg(SCH_3)_2$ and 10% for $Hg(SCH_2CH_3)_2$ (using unrelaxed structures and best basis sets). This difference in precision can be explained by the different basis set quality: $RK_{max} = 2.75$ could be reached in the second case, but only $RK_{max} = 1.75$ in the first due to its larger unit cell.

The EFG changes significantly with basis set size, and it seems that a better basis would also yield EFGs in closer agreement with experiment (see the $Hg(SCH_3)_2$ value with $RK_{max} = 3.00$).

The significant changes in the EFG values during relaxation are caused by the unphysical shortening of the Hg–S-bondlength (4.06 a.u. compared to 4.46 a.u. for crystalline $Hg(SCH_3)_2$), but shows the strong dependence of the Hg EFG on the nearest neighbour distance.

The magnitude of the EFG does not depend very much on structural details further away from the Hg atom (compare crystal with molecule), while the asymmetry parameter η does. The very limited basis set of the calculations does not allow to corroborate our expectations concerning the off-site contribution to the magnitude of the EFG (see 4.4). Comparing the η values for isolated molecules and crystals, the free molecules have a significantly larger η, probably due to the larger anisotropy in molecules compared to the more densely packed crystals.

Acknowledgements

The authors gratefully acknowledge the support of the Deutsche Forschungsgemeinschaft (grant Bu 594/9-1).

[1] D. C. Bradley and N. R. Kunchur, J. Chem. Phys. **40,** 2258 (1964).
[2] D. C. Bradley and N. R. Kunchur, Canadian Journal of Chemistry **43,** 2786 (1965).
[3] P. Blaha, K. Schwarz, P. Sorantin, and S. B. Trickey, Comput. Phys. Commun. **59,** 399 (1990). Updated WIEN95 version was used.
[4] P. Blaha, P. Dufek, K. Schwarz, and H. Haas, Hyp. Int. **97/98,** 3 (1996).
[5] T. Butz, S. Saibene, Th. Fraenzke, and M. Weber, Nucl. Instr. Meth. **A284,** 417 (1989).
[6] T. Butz, Z. Naturforsch. **51 a,** 396 (1996), and references therein.
[7] E. Wertheim, J. Amer. Chem. Soc. **51,** 3661 (1929).
[8] W. Tröger, T. Butz, P. Blaha, and K. Schwarz, Hyp. Int. **80,** 1109 (1993).
[9] B. Kohler, S. Wilke, M. Scheffler, R. Kouba, and C. Ambrosch-Draxl, Comp. Phys. Commun. **94,** 31 (1996).
[10] T. Soldner, W. Tröger, T. Butz, P. Blaha, and K. Schwarz, 1997. Z. Naturforsch. A. (this volume).
[11] T. Butz, Th. Völkel, and O. Nuyken, Chemical Physics **149,** 437 (1991).
[12] L. Hemmingsen and U. Ryde, 1995. To be submitted to J. Phys. Chem.
[13] T. Soldner, Elektrische Feldgradienten in Mercaptiden, Cadmium- und Quecksilberhalogeniden: Theorie und Experiment. Diplomarbeit, Universität Leipzig, Fakultät für Physik und Geowissenschaften, 1996.